ROS-Induced Stress Promotes Enrichment and Emergence of Antibiotic Resistance in Conventional Activated Sludge Processes

*Bharat Manna[1], Xueyang Zhou[1], and Naresh Singhal[1,2] **

[1]Department of Civil and Environmental Engineering, University of Auckland, Auckland 1142, New Zealand

[2]Water Research Centre, University of Auckland, Auckland 1142, New Zealand

*Corresponding author: n.singhal@auckland.ac.nz

Abstract

Since the Great Oxidation Event 2.4 billion years ago, microorganisms have evolved sophisticated responses to oxidative stress. These ancient adaptations remain relevant in modern engineered systems, particularly in conventional activated sludge (CAS) processes, which serve as significant reservoirs of antibiotic resistance genes (ARGs). While ROS-induced stress responses are known to promote ARG enrichment/emergence in pure cultures, their impact on ARG dynamics in wastewater treatment processes remains unexplored. Shotgun-metagenomics analysis of two hospital wastewater treatment plants showed that only 35-53% of hospital effluent resistome was retained in final effluent. Despite this reduction, approximately 30% of ARGs in CAS showed higher abundance than upstream stages, of which 22% emerged *de novo*. Beta-lactamases and efflux pumps constituted nearly 50% of these enriched ARGs. These ARGs exhibited significant correlations ($p < 0.05$) with ROS stress response genes (*oxyR*, *soxR*, *sodAB*, *katG* and *ahpCF*). The CAS resistome determined 58-75% of the effluent ARG profiles, indicating treatment processes outweigh influent composition in shaping final resistome. Proof-of-concept batch reactor experiments confirmed increased ROS and ARG levels under high dissolved oxygen (8 mg/L) compared to low oxygen (2 mg/L). Untargeted metaproteomics revealed higher expression of resistant proteins (*e.g.*, OXA-184, OXA-576, PME-1, RpoB2, Tet(W/32/O)) under elevated ROS levels. Our findings demonstrate that CAS processes actively shape effluent resistome through ROS-mediated selection, indicating that treatment processes, rather than initial wastewater composition, determine final ARG profiles. This study indicates that the emergence of ARGs needs to be considered as an integral aspect of wastewater treatment design and operation to prevent antibiotic resistance dissemination.

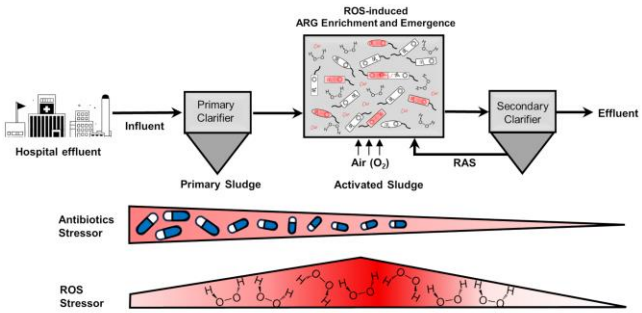

Keywords: wastewater treatment, great oxygenation event, reactive oxygen species, metagenomics, SWATH-metaproteomics

37 **Highlights**

38 • Approximately 30% of ARGs enriched in CAS versus upstream stages, of which 22%
39 emerged *de novo*

40 • Beta-lactamases and efflux pumps comprise ~50% of enriched ARGs in CAS

41 • CAS resistome shapes 58-75% of effluent ARGs, outweighing influent composition

42 • High DO levels increase ROS production and ARG abundance in CAS systems

43 • Metaproteomics confirms higher expression of resistant proteins under elevated ROS
44 levels

45

1. Introduction

Antibiotic resistance (AR) poses an escalating threat to global public health, responsible for approximately 1.27 million fatalities worldwide and contributing to almost an estimated 4·95 million (3·62–6·57) deaths associated with bacterial antimicrobial resistance in 2019 (Murray, Christopher JL, 2022). In the United States alone, infections afflict over 2.8 million individuals annually, leading to the deaths of more than 35,000 people (Centers et al., 2019). The financial burden of managing infections caused by six prevalent antibiotic-resistant bacteria (ARB) (Murray, Christopher JL, 2022) especially within healthcare settings exceeds $4.6 billion each year (Nelson et al., 2021). Antibiotic resistance is a critical One Health issue (McEwen and Collignon, 2018), profoundly affecting humans, animals, and the environment, impacting even the most fundamental resource for life: water.

The presence of antibiotic-resistant genes (ARGs) and ARBs often can be attributed to effluents from hospitals, farms, and sewage systems, illustrating the interconnectedness of human activities and the broader environmental impact of AR (Agga et al., 2015; Rowe et al., 2017). As wastewater treatment plants (WWTPs) operate at the human-environment interface, they play a crucial role in both managing and understanding the global health effects of AR (Alexander et al., 2020; Manaia et al., 2018). WWTPs receive and process diverse influents, including hospital effluents laden with high concentrations of antibiotics, ARBs, and ARGs (Y. Chen et al., 2020; Uluseker et al., 2021; Wang et al., 2022). This influx creates a potent selection pressure for ARGs and facilitates horizontal gene transfer (HGT) among bacterial communities (Karkman et al., 2018; Uluseker et al., 2021; Wei et al., 2021). Notably, hospital wastewaters harbor ARG concentrations several orders of magnitude higher than municipal wastewater (Korzeniewska et al., 2013), highlighting their alarming potential to seed and propagate resistance within WWTPs

69 treating such influents (Hocquet et al., 2016; Mehanni et al., 2023; Paulus et al., 2019).
70 Moreover, recent studies reported that different WWTP treatment processes could exhibit
71 varying impacts on ARG and ARB dynamics (Honda et al., 2023; Luo et al., 2021; Majeed et al.,
72 2021). Interestingly, the authors identified significant alteration in the ARGs composition in the
73 sludge compared to that of the influent resistome and suggested seasonality in antimicrobial use
74 to be key influencing factor behind this transition (Honda et al., 2023). A multi-omics study
75 revealed significant enrichment of both absolute and relative abundance of specific resistance
76 genes in CAS resistome compared to influent, particularly those conferring resistance to ARGs
77 drug classes (multidrug, beta-lactam, aminoglycoside, tetracycline, vancomycin etc.), suggesting
78 bacterial community composition and biomass concentration as key factors (Ju et al., 2019).
79 Moreover, another study showed that while the overall ARGs abundance decreased during 11 out
80 of 12 WWTPs, there were instances of specific ARGs being enriched in the effluents (Garner et
81 al., 2024). Many other reports also identified CAS processes as potential hotspots for ARG
82 enrichment (Bengtsson-Palme et al., 2016; Guo et al., 2017; Liu et al., 2018, 2019; Majeed et al.,
83 2021; Petrovich et al., 2020). These enriched ARGs in CAS contribute significantly to the
84 effluent resistome which is disseminated into the receiving environment (Honda et al., 2023; Ju
85 et al., 2019; Majeed et al., 2021). However, the specific mechanisms driving the enrichment and
86 emergence of ARGs within CAS processes remain poorly understood. Consequently,
87 understanding the underlying mechanisms behind the emergence of ARGs in CAS processes has
88 become an urgent need.
89 While antibiotics are relatively recent human inventions, microbes have developed resistance
90 mechanisms over thousands of years through their continuous evolutionary struggle for survival
91 (Dcosta et al., 2011). To understand bacterial resistance mechanisms, the perspective of oxygen

92 on Earth provides a critical evolutionary context. Prior to the Great Oxidation Event (GOE)
93 around 2.4-2.1 billion years ago, Earth's atmosphere was essentially oxygen-free, and early life
94 thrived in a reducing condition (Lyons et al., 2014). The dramatic rise of oxygen through
95 photosynthesis represented the first major oxidative stress that organisms had to adapt to, driving
96 the evolution of cellular mechanisms to cope with oxygen toxicity and its reactive species
97 (ROS). Recent evidence suggests a unifying mechanism behind the action of many bactericidal
98 antibiotics, where ROS generation plays a key role behind lethality (Dwyer et al., 2009; Lam et
99 al., 2020; Van Acker and Coenye, 2017). ROS like hydrogen peroxide (H_2O_2), hydroxyl radical
100 ($OH^{\cdot}$), singlet oxygen ($^1O_2$), and superoxide anion (O_2^-) are inherent byproducts of bacterial
101 aerobic respiration (Imlay, 2019, 2003). Furthermore, ROS-mediated killing can trigger a
102 secondary stress response beyond the initial antibiotic-induced damage, involving factors like
103 activation of response regulators (*e.g.*, *ArcA*), metabolic reprogramming of the TCA cycle, and
104 disruption of the nucleotide pool with increased ATP demand (Li et al., 2021) (Figure S1). To
105 counter this oxidative stress and survive, bacteria have evolved diverse antioxidant defenses
106 through metabolic remodeling (Li et al., 2021). However, bacterial efforts to develop ROS
107 tolerance often come at a cost. The increased oxidative stress can lead to direct DNA damage,
108 potentially triggering novel mutations, and ultimately contributing to the emergence of AR
109 (Ariza et al., 1994; Jin et al., 2018; Mandsberg et al., 2009; Qi et al., 2023). Since ROS are
110 common to both antibiotic action and bacterial stress responses, resistance to ROS could be a key
111 shared characteristic underlying ARG development. We recently showed that ROS stress has
112 been linked to ARGs proliferation in freshwater microbial communities (Manna et al., 2024).
113 These ancient adaptations to oxidative stress remain fundamental to how modern
114 microorganisms handle ROS in highly aerated wastewater treatment systems. The significance of

115 ROS in CAS processes can be attributed to the constant aeration inherent to these systems, which
116 creates a unique environment characterized by high dissolved oxygen (DO) levels and,
117 consequently, elevated ROS generation. While existing research hints at the connection between
118 ROS and ARG emergence in the context of WWTP, it primarily focuses on lab experiments and
119 specific antibiotics or stressors. One study observed a significant increase in antibiotic resistance
120 in *Escherichia coli* exposed to aeration tanks compared to primary or final sedimentation tanks
121 (Sulfikar et al., 2018). Another study linked triclosan-induced oxidative stress to a rise in ARGs,
122 particularly tetracycline and multidrug resistance genes (Tan et al., 2021). Similarly, ROS
123 generated by phenolic compounds have been proven to promote resistance through increased
124 membrane permeability and HGT (Ma et al., 2021). Moreover, antidepressant fluoxetine induced
125 resistance to multiple antibiotics (*e.g.*, fluoroquinolone, aminoglycoside, β-lactams, tetracycline
126 and chloramphenicol) in *Escherichia coli* via ROS-mediated mutagenesis (Jin et al., 2018).
127 Despite these findings, the critical question of whether aeration-induced ROS in real-world
128 WWTPs shape the multifaceted resistome in CAS processes, remains unanswered.
129 Building on this evolutionary and mechanistic foundation, we present a comprehensive
130 investigation of how aeration-induced oxidative stress shapes antibiotic resistance in full-scale
131 CAS processes. By combining whole-genome shotgun metagenomics analysis from two WWTPs
132 treating hospital effluents and untargeted metaproteomics from controlled batch reactor
133 experiments, we unravel the relationship between DO levels, ROS generation, and ARG
134 dynamics, providing unprecedented insights into how oxidative stress drives resistance
135 development in CAS processes.

136 **2. Materials and methods**

137 **2.1. Sample data collection**

In this work, we considered paired-end shotgun metagenomics samples obtained using a HiSeq 2500 instrument from two full-scale WWTPs processing university hospital effluents in Göttingen ($WWTP_{Gö}$), and Greifswald ($WWTP_{Gw}$), Germany (Schneider et al., 2020). The samples were collected from five different stages (abbreviated as S) from both the WWTPs, *i.e.*, S1: Hospital effluent (a storage tank next to the university hospital), S2: WWTP Influent, S3: Primary Sludge, S4: conventional activated sludge (CAS), and S5: WWTP effluent as described elsewhere (Schneider et al., 2021, 2020). The details of the sample names, and NCBI SRA accession used in this study, can be found in Table S1 and Table S2. The raw metagenomes can be accessed in the NCBI Sequence Read Archive under the BioProject accession number PRJNA524094 (Schneider et al., 2021).

2.2. Metagenomics Analysis

We performed preprocessing steps to eliminate low-quality sequences using Trimmomatic v0.39 (Bolger et al., 2014) with specific quality thresholds (Manna et al., 2024). For metagenomic analysis, we employed the SqueezeMeta v1.5.2 pipeline (Tamames and Puente-Sánchez, 2019). The read statistics per sample are provided in Table S1 and Table S2. Co-assembly was performed using Megahit v1.2.9 (D. Li et al., 2015). Within the SqueezeMeta pipeline, Barrnap v0.9 (Seemann, 2014) tool was used for predicting RNAs, while Prodigal v.2.6.3 (Hyatt et al., 2010) was utilized for predicting ORFs. Moreover, the Comprehensive Antibiotic Resistance Database (Alcock et al., 2020) release 3.2.4 was used for annotating the ARGs using Diamond v.2.0.14 (Buchfink et al., 2014) with sequence identity of 70% and e-value threshold of 1×10^{-3} (Manna et al., 2024; Petrovich et al., 2020). ARG abundances were normalized using the 16S-rRNA gene abundance as per previous report (B. Li et al., 2015). ARGs conferring resistance to more than one antibiotic was classified as ‘multidrug resistant’ (MDR). Similarity searches

against Kyoto Encyclopedia of Genes and Genomes (Kanehisa and Goto, 2000), were performed for functional assignments of ORFs. The metagenomics data was analyzed using the SQMtools v1.6.3 R package (Puente-Sánchez et al., 2020).

2.3. Bioinformatics Analysis and Visualization

To assess the diversity of ARG composition across the different treatment stages, we calculated a Bray-Curtis dissimilarity matrix with PERMANOVA to determine the significance of clustering, using MicrobiomeAnalyst v2.0 (Dhariwal et al., 2017). A heatmap was plotted to visualize changes in the abundance of each ARG, utilizing a z-score with TBtools v2.007 (C. Chen et al., 2020). Furthermore, differentially abundant (enriched/emerged) ARGs in CAS (S4) were identified using EdgeR v.4.4.0 (Robinson Mark et al., 2010) with an adjusted *p*-value cutoff of 0.05. The correlation between ROS stressor genes and differentially abundant ARGs was performed using a Mantel test (p-value < 0.05) using OmicStudio tools v1.41.0 (Lyu et al., 2023). Graphics were generated using the ggplot2 v3.5.1 (Wickham, 2011) package in R (R Core Team, 2022) version 4.2.1.

2.4. Batch reactor experiments with different DO levels

To validate our metagenomics-based findings of higher ROS generation under more oxidative stress leading to increased ARGs, we performed batch reactor experiments with CAS samples under low (2 mg/L) and high (8 mg/L) DO levels. The CAS samples were obtained from the Māngere WWTP in Auckland, New Zealand. The experiments were conducted in reactors (n = 3 biological replicates per condition) with a capacity of 1 L, at a temperature of 20 °C for 48 hours. Composition of the synthetic wastewater is provided in Table S3 and Table S4. Detailed methodology for ROS measurement, DNA extraction for metagenomics analysis and untargeted metaproteomics analysis are provided in Supplementary Methods. The raw metagenome samples

184 from these experiments can be accessed in the European Nucleotide Archive under the
185 BioProject accession number PRJEB74089 as provided in Table S5.

186 **2.5. SWATH-MS based quantitative Metaproteomics Analysis**

187 Untargeted metaproteomic analysis was performed on activated sludge samples to characterize
188 microbial protein expression under the two DO conditions. Proteins were extracted using SDS-
189 based lysis buffer, followed by sonication and TCA-acetone precipitation. Tryptic-digested
190 peptides were analyzed using a NanoLC 400 UPLC (Eksigent, USA) system coupled to a
191 TripleTOF 6600 mass spectrometer (Sciex, USA). Protein identification using
192 MetaProteomeAnalyzer v3.4 (Muth et al., 2015) with X-tandem revealed 1,110 distinct proteins
193 for functional analysis. Detailed methodology is available in Supplementary Methods. The
194 metaproteomics data has been submitted to ProteomeXchange Consortium with the dataset
195 identifier PXD044490.

196 **3. Results and Discussion**

197 **3.1. Comparison of ARG abundances across different treatment stages**

198 In this study, we systematically analyzed and compared metagenomic samples from various
199 stages of wastewater treatment processes to assess changes in the resistome profile. These stages
200 included hospital effluents (S1), WWTP influent (S2), primary treatment (S3), CAS (S4), and
201 WWTP effluents (S5) (Figure 1a). Our findings showed a considerable decrease in total ARG
202 abundances at different stages of $WWTP_{Gö}$ compared to the hospital effluents: 54.17% in S2,
203 53.38% in S3, 78.69% in S4, and 83.30% in S5 (Figure 1b). Moreover, 69.50%, 68.42%,
204 46.59%, and 35.14% of the ARGs detected in S1 were retained in S2, S3, S4 and S5,
205 respectively (Figure S2a).

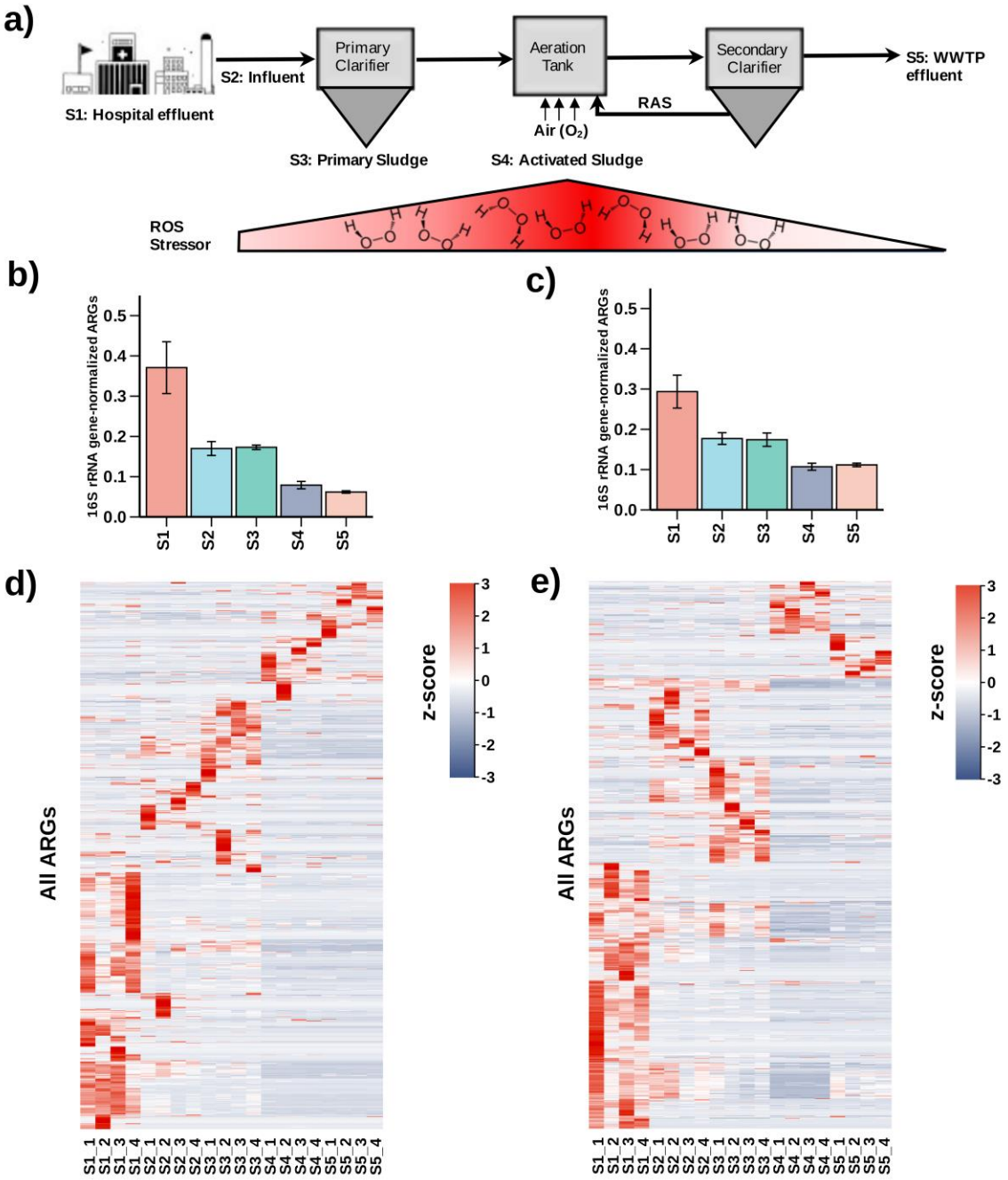

Figure 1. Alteration of ARG abundance across different WWTP stages. (a) Schematic representation of the WWTP stages studied, including S1: Hospital effluent, S2: WWTP influent, S3: Primary sludge, S4: Activated sludge, and S5: WWTP effluent. The variation in ROS stressor levels across these stages is depicted below. (b) and (c) show the total relative ARG abundance at each stage for $WWTP_{Gö}$ and $WWTP_{Gw}$, respectively. Heatmaps display the trend of change in each ARG relative abundance across the stages in (d) $WWTP_{Gö}$ and (e) $WWTP_{Gw}$ with a prominent set of enriched (or emerged) ARGs (red) in both S4 and S5. RAS: Recycled activated sludge.

213 A similar analysis conducted in the $WWTP_{Gw}$ also revealed a reduction in ARG abundances of
214 39.70% in S2, 40.65% in S3, 63.55% in S4, and 61.99% in S5, compared to S1 (Figure 1c). The
215 numbers of ARGs detected in S1 were retained by 73.14% in S2, 67.55% in S3, 31.52% in S4,
216 and 53.42% in S5 (Figure S2c). The highest abundance of ARGs was observed in the hospital
217 effluent (S1) for both WWTPs, which is expected due to the prevalent use of antibiotics in
218 hospital settings, leading to a higher presence of ARGs. Across the treatment stages, a consistent
219 trend of ARG reduction was noted, indicating the effectiveness of the WWTP processes in
220 decreasing the overall ARG abundance in the effluent (S5). This pattern of ARG reduction in
221 CAS and effluents are in agreement with previous metagenomics-based studies (Bengtsson-
222 Palme et al., 2016; Honda et al., 2023; Lira et al., 2020).
223 Furthermore, the diversity of resistome profiles across various stages of the $WWTP_{Gö}$ and
224 $WWTP_{Gw}$ was evaluated using principal coordinate analysis (PCoA) with a Bray-Curtis
225 dissimilarity matrix (Figure S2b, d). The PCoA demonstrated clear clustering of resistomes
226 corresponding to the five treatment stages. Significant separation observed (R^2: 0.79329,
227 PERMANOVA F-value: 14.392, *p*-value: 0.001) in $WWTP_{Gö}$, indicating distinct ARG profiles
228 at each treatment stage. Similarly, $WWTP_{Gw}$'s resistome profiles were markedly segregated
229 demonstrating substantial differentiation (R^2: 0.83563, PERMANOVA F-value: 19.064, *p*-value:
230 0.001). The PCoA results showed that the resistomes from S1, S2, and S3 stages clustered
231 closely, suggesting similar ARG profiles, possibly due to the direct contribution of hospital
232 effluent to the influent. In contrast, samples from the CAS (S4) and treated effluent (S5) stages
233 were distinctly separate from the preceding stages. This delineation reflects a significant
234 transition in the ARG profile, attributable to the biological processes and selection pressure
235 within the activated sludge system and secondary clarifiers. Notably, the effluent resistome

236 consisted of 58.42% and 75.58% of the CAS resistome in the $WWTP_{Gö}$ and $WWTP_{Gw}$,
237 respectively, indicating a substantial overlap between the systems. The distinct clusters for the
238 S4 and S5 stages also suggest that the treatment process, rather than initial wastewater
239 composition, determines final effluent ARG profiles, with potential environmental implications
240 upon its release. Similar variations in resistome in influent, activated sludge and effluent have
241 been reported in previous studies (Honda et al., 2023; Majeed et al., 2021).
242 In addition to the overall trend analysis, a detailed heatmap of all ARGs based on normalized
243 abundance (z-scores) was generated to further elucidate the specific changes in ARG profiles at
244 each treatment stage, with a focus on the CAS (S4) process (Figure 1d, e). The heatmap
245 illustrated that while some ARGs were consistently abundant across all stages, others were more
246 stage specific. This abundance pattern reinforces the notion of stage-specific selective pressures
247 and microbial community dynamics shaping the ARG profile. Interestingly, despite the general
248 trend of decreasing total ARG abundance (Figure 1b, c), certain ARGs exhibited notable
249 persistence and remarkable enrichment/emergence in the CAS stage (S4) in both the WWTPs
250 (Figure 1d, e). This relative enrichment of ARGs in the CAS was previously reported using
251 combined metagenomics and metatranscriptomics study (Ju et al., 2019).

252 **3.2. Identifying the enriched and emerged ARGs in the CAS process**

253 To enhance our understanding of the enriched or emerged ARGs within the CAS process, we
254 conducted a detailed analysis of ARGs that were differentially more abundant in CAS than in the
255 upstream stages. Specifically, in the $WWTP_{Gw}$ facility, we observed that 111, 115, and 116
256 ARGs exhibited significantly (FDR < 0.05) higher abundance in CAS when compared to S1, S2,
257 and S3, respectively, as illustrated in Figure 2a. Similarly, for the $WWTP_{Gö}$ facility, 152, 138,
258 and 114 ARGs were found to be more abundant in CAS relative to the same comparator stages

259 (Figure S3a). Additionally, certain ARGs were identified as being significantly more abundant in
260 S4 compared to all other stages (S1, S2, and S3), with some ARGs being uniquely abundant to
261 specific treatment stages (Figure S4 and Supplemental Data 1). To facilitate downstream
262 analyses, we compiled a list of ARGs that were significantly abundant in the CAS process,
263 selecting those genes that displayed a higher average abundance in CAS compared to all
264 preceding treatment stages. This analysis yielded a total of 116 (29.59%) and 94 (36.43%) highly
265 abundant ARGs for $WWTP_{Gö}$ and $WWTP_{Gw}$, respectively, as detailed in Supplemental Data 2a.
266 Notably, 22.22% ($WWTP_{Gö}$) and 21.88% ($WWTP_{Gw}$) of the abundant ARGs were not detected
267 at any of the upstream stages, suggesting they emerged under the selection pressure of the CAS
268 process (Supplemental Data 2b). These emerged ARGs exhibited resistance to aminoglycoside
269 (*AAC(3)-IIIc*, *AAC(6')-Iih*), beta-lactam (*OXA-34*, *OXA-660*, *OXA-4*, *GOB-3*, *GOB-4*, *IDC-2*,
270 *IMP-1*, *IMP-13*, *IMP-28*), rifamycin (*iri*, *arr-1*), tetracycline (*tap*, *tet(V)*), glycopeptide (*vanD*,
271 *vanI*), and other antibiotics. Additionally, among the enriched ARGs in both WWTPs were those
272 belonging to various beta-lactamases, such as *OXA* (including *OXA-45*, *OXA-101*, *OXA-129*,
273 *OXA-198*) beta-lactamases. These ARGs confer resistance to antibiotics like carbapenems,
274 cephalosporins, and penams, highlighting a significant selection pressure for beta-lactam
275 resistance. This is especially concerning given the extensive use of beta-lactam antibiotics and
276 the potential for these resistance mechanisms to spread into the environment. Furthermore, we
277 identified multiple ARGs conferring resistance to other antibiotic classes, including tetracycline
278 (*tet(35)*, *tet(49)*, *tet(G)*, *tet(T)* etc.), glycopeptide (*vanC*, *vanF*, *vanS_in_vanC_cl*, etc.), and
279 aminoglycoside (*AAC(3)-Id*, *AAC(6')-32*, *AAC(6')-Ic*, *AAC(6')-IIa*, *AAC(6')-IIb*, *AAC(6')-IIc*,
280 etc.), among others. Resistance to rifamycin (*rpoB2*, *Bado_rpoB_RIF*, *Nfar_rox*, *rphA*, *rphB,*),
281 macrolide (*EreB*, *mphA*), fluoroquinolone (*QepA4*, *QnrS6*, *QnrS8*), and sulfonamide (*sul2*, *sul4*)

282 antibiotics were also observed, alongside ARGs resistant to multiple antibiotics, such as *AxyY*,
283 *efrB*, *MexF*, *mexP*, *mexQ*, *mexY*, *opmE*, *smeE*, and more, as provided in Supplemental Data 2a.
284 Amongst the enriched/emerged ARGs, beta-lactamases (WWTPGö: 24.14%, WWTPGw:
285 25.53%) and efflux pumps (WWTPGö: 23.28%, WWTPGw: 27.66%) represented the
286 predominant resistance mechanisms in both WWTPs. Our recent study also demonstrated that
287 oxidative stress conditions could exacerbate ARG proliferation, particularly efflux pump genes
288 (Manna et al., 2024). Consistent with our observations, a significant enrichment of various
289 resistance genes, including those encoding for beta-lactamases, macrolides, and tetracyclines,
290 was identified in recirculated activated sludge in comparison to primary sludge (Bengtsson-
291 Palme et al., 2016). This enrichment was suggested due to the selective pressure within the
292 wastewater treatment facility. Similarly, previous research documented an escalation in the
293 relative abundance of a wide array of ARGs, spanning multiple drug classes such as beta-
294 lactamases, aminocoumarins, glycopeptides, rifamycins, and sulfonamides, from influent to
295 effluent in a conventional WWTP (Majeed et al., 2021). Furthermore, another study reported an
296 increase in both the transcript and gene abundance of various ARG classes, including Multidrug,
297 beta-lactamases, aminoglycosides, tetracyclines, trimethoprim, and vancomycin, in secondary
298 effluent compared to the influent of post-primary clarifiers (Ju et al., 2019). Additionally, it was
299 found that aerobic biomass exhibited a higher overall abundance of ARGs compared to
300 anaerobic and anoxic biomass, with a notable increase in effluent abundances of fluoroquinolone
301 and tetracycline ARGs (Petrovich et al., 2020). These observations underscore the diverse
302 spectrum of resistant ARGs emerging within the CAS process, indicating that while the CAS
303 process effectively reduces the overall ARG load, it also inadvertently facilitates the proliferation
304 (enrichment and emergence) of multiple concerning ARGs.

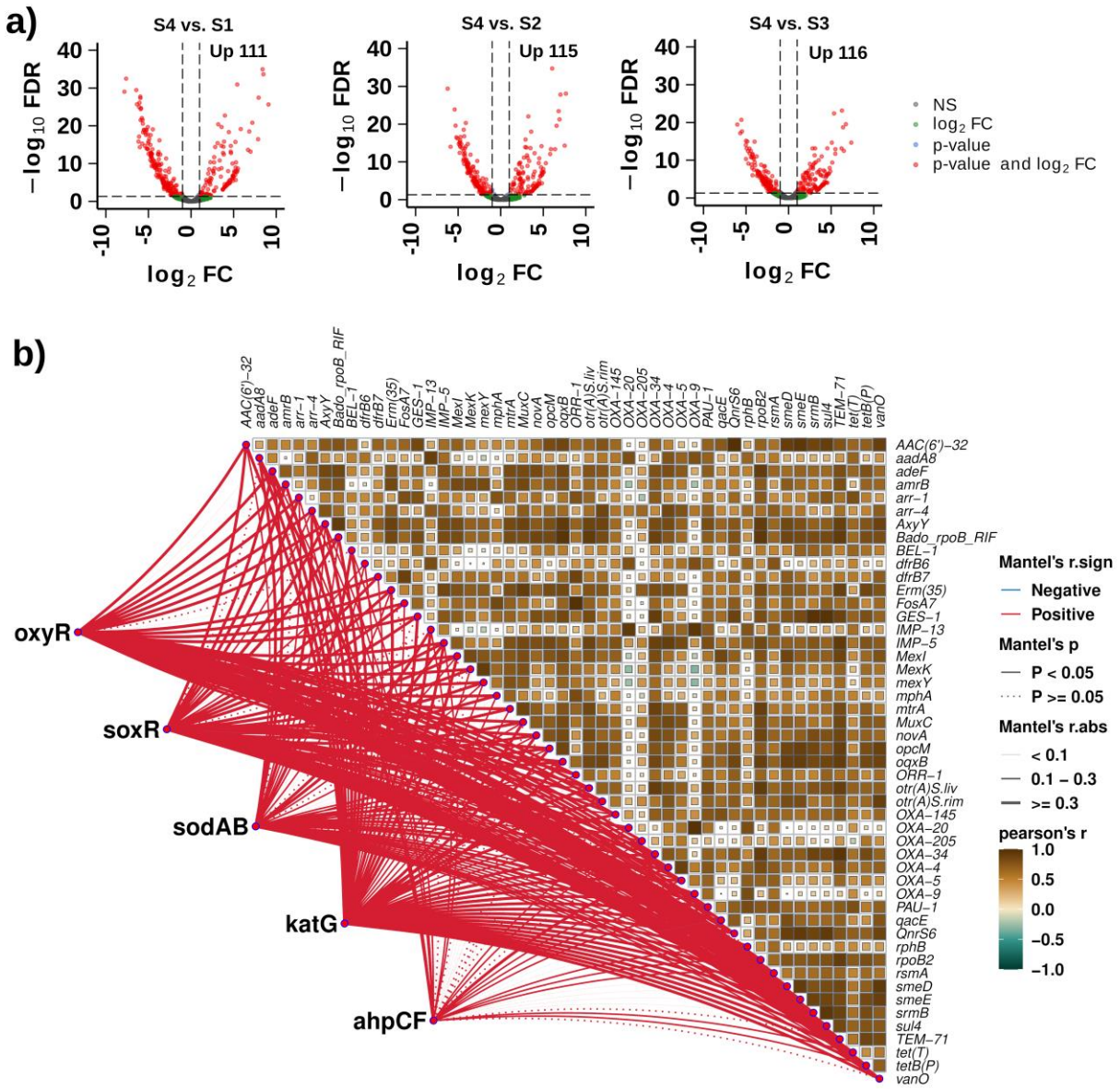

Figure 2. Differentially enriched (or emerged) ARGs and their correlation network with ROS stressors in the CAS process. a) Volcano plots illustrate the differentially abundant ARGs in the CAS stage compared to S1, S2, and S3 in the $WWTP_{Gw}$ ($log_2FC \geq 1$, FDR < 0.05). b) A network analysis depicting the correlations between selected enriched/emerged ARGs and ROS stress response genes in CAS process in $WWTP_{Gw}$.

3.3. Assessing the correlation between the ROS stressors and enriched or emerged ARGs

To further assess previously established connections between oxidative stress and antibiotic resistance, we analyzed correlations between ROS-response genes and the enriched/emerged ARGs detected in the CAS systems of both WWTPs. We focused on five crucial ROS-related

genes (Seo et al., 2015): two transcription factors, *oxyR* and *soxR*, which play key roles in the cellular response to oxidative stress, and three genes encoding enzymes that help detoxify ROS, namely *sodAB* (Superoxide dismutase), *katG* (Catalase-peroxidase), and *ahpCF* (alkyl hydroperoxide reductase). Notably, previous reports revealed *oxyR* (Lau et al., 2005; Wei et al., 2012) and *soxRS* (P. Wang et al., 2020) contributed to virulence in *E. coli*, *Pseudomonas aeruginosa*, and *Salmonella enterica*. Our analysis revealed a significant correlation between these ROS stress response genes and numerous ARGs in both WWTPs (Figure 2b, Figure S3b, Supplemental Data 3). Specifically, in the $WWTP_{Gö}$, the number of ARGs positively correlated with each ROS stressor were *oxyR* (7), *soxR* (35), *sodAB* (22), *katG* (31), and *ahpCF* (17). Meanwhile, in $WWTP_{Gw}$, the numbers of ARGs linked to the same stressors were *oxyR* (60), *soxR* (49), *sodAB* (52), *katG* (79), and *ahpCF* (17). In the case of $WWTP_{Gö}$, we identified several ARGs showing correlations with different combinations of ROS stressors (Figure S5a). Most notably, 4 ARGs (*AAC(6')-IIb*, *lmrC*, *OXA-4*, and *QepA4*) correlated with all ROS stressors examined. The largest individual correlations were observed with *soxR*, which correlated with 10 ARGs, including tetracycline resistance genes (*tet(T)*, *tet(W/32/O)*), and various others (*Abau_AbaQ*, *dfrG*, *HelR*, *mexN*, *otr(A)S.liv*, *TriC*, *vgaALC*). Furthermore, a significant group of 6 ARGs, including metallo-beta-lactamases (*IMP-13*, *IMP-28*), beta-lactamases (*OXA-9*), and others (*aadA8*, *arr-1*, *vanS_in_vanO_cl*), showed correlation specifically with both *sodAB* and *katG*, indicating a potential link between these antioxidant enzymes and antibiotic resistance mechanisms. Additional notable correlations were observed with *katG* alone, which correlated with 9 ARGs, including various resistance mechanisms (*adeF*, *dfrB2*, *mphA*, *MYO-1*, *OXA-198*, *smeE*, *vanD*, *vanS_in_vanP_cl*, *vgaD*), suggesting a broad spectrum of antibiotic resistance mechanisms being influenced by oxidative stress responses. Besides, within the $WWTP_{Gw}$, 10

337 ARGs were correlated with all ROS stressors, including genes responsible for multidrug
338 resistance (*adeF*), beta-lactamase activity (*OXA-4*, *OXA-5*, *PAU-1*, *IMP-5*), tetracycline
339 resistance (*tet(T)*, *tetB(P)*), and rifamycin resistance (*rpoB2*), among others (*rsmA*, *arr-4*) (Figure
340 S5b). Additionally, a noteworthy observation was the correlation of a considerable number of
341 ARGs with multiple ROS stressors, specifically 24 ARGs correlating with *soxR*, *oxyR*, *sodAB*,
342 and *katG* (including *AxyY*, *MuxC*, *OXA-145*, *mexY*, and others), and 11 ARGs correlating with
343 *soxR*, *oxyR*, and *katG* (including *mtrA*, *vanD*, *mphA*, and others). Comparative analysis of both
344 WWTPs revealed many common ARGs showing correlations with various ROS stressors,
345 including genes encoding beta-lactamases (*OXA-4*, *PAU-1*), tetracycline resistance (*tet(T)*,
346 *tetA(60)*), rifamycin resistance (*rpoB2*), and various multidrug resistance mechanisms (*adeF*,
347 *AxyY*, *smeE*), suggesting shared patterns of ROS-mediated antibiotic resistance regulation across
348 different wastewater treatment environments. These observed patterns align with and extend
349 previous research findings in the field. For instance, studies with *Escherichia coli* K12
350 demonstrated that strains resistant to multiple antibiotics (chloramphenicol, amoxicillin and
351 tetracycline) produced significantly higher levels of ROS compared to the wild-type (Jin et al.,
352 2018). Additionally, the resistant strains also exhibited significant overexpression of ROS
353 scavengers including *sodA* and *ahpF*. A recent study showed that exposure to bactericidal
354 antibiotics (amoxicillin, enrofloxacin, and kanamycin) increased ROS production in the *oxyR*
355 knocked out *E. coli* compared to the wild-type (Qi et al., 2023). Moreover, heme induced
356 electron transport chain enhanced the ROS production, leading to *de novo* acquired resistance in
357 *Lactobacillus lactis* (Qi et al., 2023). These reports support our findings on the pattern of
358 correlations and underscore the potential link between ROS stressors and ARG emergence. A
359 notable aspect of our findings is the identification of common and unique ARGs across different

360 ROS stressors. Certain ARGs appear frequently across multiple ROS stressor correlations,
361 suggesting that these ARGs might be more universally responsive to ROS-induced stress. In
362 contrast, unique ARGs correlating with specific ROS stressors indicate targeted responses to
363 particular oxidative stress conditions. Thus far, through meticulous examination of ROS stressor
364 genes and their correlations with differentially enriched ARGs in the CAS aeration process, we
365 uncovered patterns suggesting ROS as an instrumental factor in driving ARG
366 enrichment/emergence.

367 **3.4. Experimental support for increased ARG abundance and ROS under high DO**

368 To investigate the mechanistic relationship between ROS and ARG enrichment/emergence
369 within the CAS process, we conducted batch reactor experiments using CAS samples from the
370 Māngere WWTP (Auckland, New Zealand). This experimental setup was designed to simulate
371 the oxidative conditions characteristic of the CAS process, with specific emphasis on DO
372 concentration variations. Our experimental design incorporated two distinct DO concentrations:
373 DO2 (2 mg/L) and DO8 (8 mg/L), enabling assessment of ROS generation under elevated DO
374 conditions. Quantitative analysis revealed mean H_2O_2 concentrations of 32.05 ± 2.08 μM and
375 38.38 ± 0.86 μM for DO2 and DO8 conditions, respectively (Figure 3a). The DO8 treatment
376 yielded significantly higher H_2O_2 production compared to DO2 ($p < 0.05$). Analysis of oxidative
377 stress response genes (*soxR*, *oxyR*, *sodAB*, *katG*, and *ahpCF*) demonstrated consistent
378 upregulation under DO8 conditions (Figure 3b), indicating systematic adaptation to elevated
379 ROS levels associated with higher DO concentrations. Resistome profiling revealed ARG
380 patterns consistent with those observed in both $WWTP_{Gö}$ and $WWTP_{Gw}$ CAS systems (Figure
381 S6a, b). The prevalent ARG classes encompassed resistance to aminocoumarin antibiotics,
382 aminoglycosides, beta-lactams (including carbapenems, cephalosporins, penams),

383 fluoroquinolones, macrolides, tetracyclines, peptide antibiotics, rifamycins, and sulfonamides
384 (Figure S6c). Differential abundance analysis identified 11 significantly enriched ARGs under
385 DO8 conditions (Figure 3c), including beta-lactamases (*OXA-34*), sulfonamide resistance (*sul4*),
386 tetracycline resistance (*tet(43)*, *tet(W/32/O)*), rifamycin resistance (*Bado_rpoB_RIF*, *rphA*), and
387 MDR (*mexQ*).

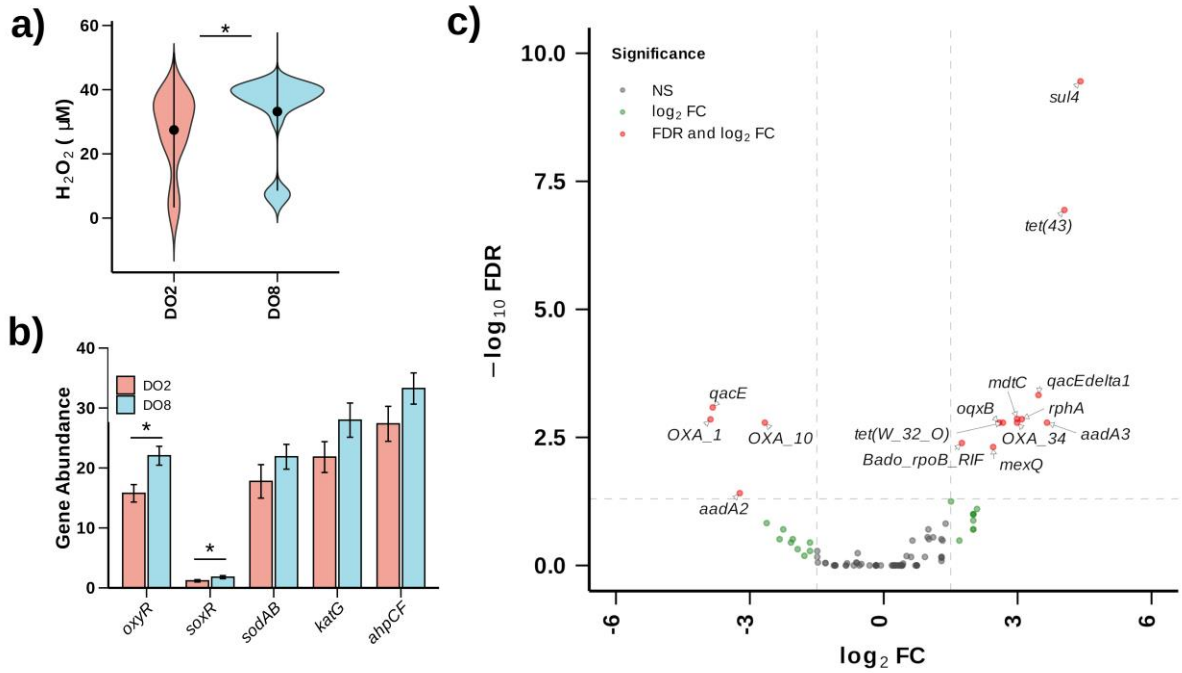

388

389 **Figure 3.** DO concentration influences ROS generation and ARG abundance. a) Violin plots showing H_2O_2
390 concentrations under DO2 (2 mg/L) and DO8 (8 mg/L) conditions (*$p < 0.05$, paired t-test). b) Relative abundance
391 of oxidative stress response genes under DO2 and DO8 conditions. c) Volcano plot of differentially abundant ARGs
392 comparing DO8 versus DO2 conditions ($log_2FC \geq 1.5$, $FDR < 0.05$).

393 To establish causality beyond correlation and verify protein expression, we performed untargeted
394 SWATH metaproteomics analysis. Results demonstrated enhanced expression of several ARGs
395 under DO8 conditions, including beta-lactamases (OXA-184, OXA-576, PME1), rifamycin
396 resistance (RpoB2), tetracycline resistance (Tet(W/32/O)), and aminoglycoside resistance
397 (AAC(6')-Ia) (Figure 4). While some proteins showed elevated expression under DO2 conditions

398 (Bpse_Omp38, K15582), others exhibited comparable expression levels across both conditions
399 (BUT-1, JOHN-1, OXA-153). These findings provide mechanistic insights into ARG dynamics
400 within CAS processes. The correlation between elevated ROS levels under high DO conditions
401 and upregulation of oxidative stress response genes support that increased ROS production,
402 resulting from intensive aeration in CAS systems, may contribute to ARG emergence and
403 persistence.

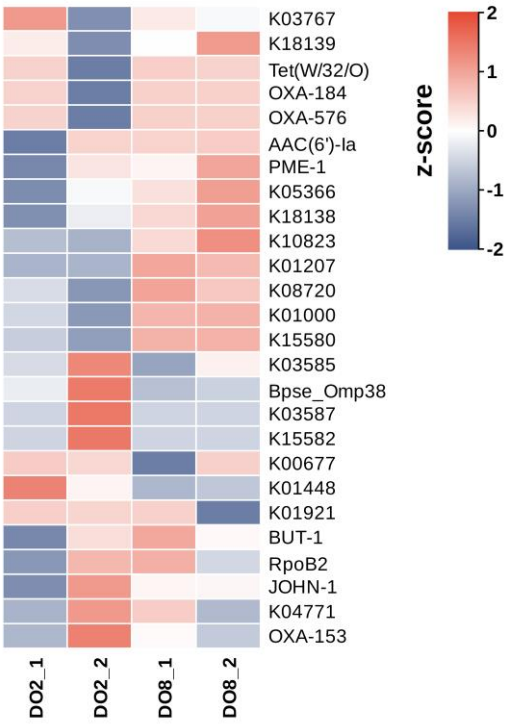

404

405 **Figure 4.** Heatmap with the protein expression of ARGs under DO2 and DO8 conditions measured by SWATH-MS
406 based metaproteomics analysis. The protein names refer to the ARGs from CARD and KEGG orthologs.

407

408 **3.5. Mechanism of ROS-induced ARG enrichment/emergence in CAS**

409 Sublethal concentrations of endogenous ROS can trigger a series of direct or indirect cellular
410 responses that may contribute to the enrichment/emergence of ARGs in the CAS process (Li et
411 al., 2021). These responses include the activation of transcriptional regulators, expression of
412 oxidative defense enzymes, metabolic adaptations, DNA damage, activation of efflux pumps,

413 cell damage, and increased permeability and transformation potential (Figure S1). Firstly,
414 enhanced expression of transcription factors like *oxyR* and *soxRS* facilitate the production of
415 ROS-scavenging enzymes such as superoxide dismutase, catalase, thioredoxins and others
416 (Imlay, 2008). In both the $WWTP_{Gö}$ and $WWTP_{Gw}$ CAS processes, we observed a high
417 abundance of these transcription factors and ROS scavengers (Figure 5 a,b). Secondly, ROS
418 stress can disrupt the TCA cycle, leading to hyperactivation of respiration, as seen in certain
419 antibiotic treatments (Kohanski et al., 2008). Previous reports also suggested the disruption of
420 the nucleotide pool, leading to the increase of ATP demand elevating TCA cycle activity and
421 cellular respiration under quinolones treatments (Yang et al., 2019). This disruption may trigger
422 metabolic adaptations, such as activating the glyoxylate shunt (GS) (Lemire et al., 2017) to
423 reduce oxidative burden or redirecting flux to the PPP for increased NADPH production,
424 supporting antioxidant defense systems (Christodoulou et al., 2018). Our comparative analysis
425 revealed an higher abundance of genes involved in these metabolic pathways, ATP and NADPH
426 production, and consumption in the CAS system compared to other treatment processes (Figure 5
427 a,b). Moreover, sublethal ROS levels can cause DNA damage and potential mutations,
428 facilitating the emergence of *de novo* antibiotic resistance (Qi et al., 2023). Notably, DNA repair-
429 related genes were abundant in the CAS processes at both WWTPs. We also identified several
430 ARGs in the CAS process that were not detected in the upstream processes of both WWTPs
431 (Supplemental Data 2b). This indicates that ROS-induced mutations could be responsible for
432 their emergence. As a secondary defense, bacteria activate multidrug efflux pumps to expel
433 antibiotics from the cell, promoting antibiotic tolerance. The abundance of multidrug efflux
434 pump genes was high in the CAS processes (Figure 5 a,b). Additionally, oxidative damage can
435 weaken the bacterial cell envelope, potentially leading to the release of ARGs into the

environment. This process, coupled with enhanced transformation capabilities under oxidative stress, increases the uptake of foreign DNA, including ARGs, through HGT. Increased cell permeability can promote the uptake of foreign ARGs and eDNA through transformation (Y. Wang et al., 2020). Previous reports suggested that *Streptococcus* sp. released eDNA under H_2O_2 stress (Itzek et al., 2011). A recent report revealed that phenolic compounds can promote ROS-induced increased cell permeability and HGT (Ma et al., 2021). These simultaneous events occurring in the CAS process under oxidative stress conditions may play a significant role in enriching ARGs or helping ARG emergence. Overall, the proposed mechanisms by which ROS can contribute to ARG enrichment/emergence in the CAS process include activation of oxidative stress responses and metabolic adaptations, DNA damage and *de novo* resistance development, increased efflux pump activity, and enhanced cell permeability promoting horizontal gene transfer facilitated by oxidative damage. This multifactorial process underscores the complex interplay between oxidative stress and antibiotic resistance in the CAS process.

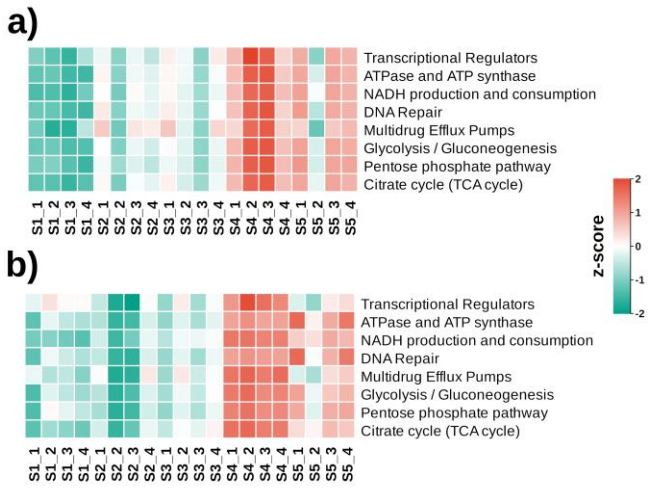

Figure 5. Heatmap illustrating the change in gene abundances associated with the cellular processes across various stages of the (a) $WWTP_{Gö}$, and (b) $WWTP_{Gw}$.

4. Conclusions

453 Our findings reveal a crucial paradox in CAS processes: while they effectively reduce overall
454 ARG loads from hospital wastewater (retaining only 35-53% in effluent), they simultaneously
455 create conditions that promote enrichment and emergence of specific ARGs. The demonstration
456 that 30% of ARGs in CAS show higher abundance, with 22% of these enriched ARGs emerging
457 *de novo*, challenges the traditional view of treatment efficiency. Beta-lactamases and efflux
458 pumps, constituting nearly 50% of enriched ARGs, highlight the selective pressures within CAS
459 systems. Most significantly, our finding that CAS resistome determines 58-75% of effluent ARG
460 profiles indicates that treatment processes, rather than influent composition, shape the final
461 resistome. The mechanistic link between ROS generation and ARG proliferation, validated
462 through batch experiments, demonstrates how ancient oxidative stress responses continue to
463 influence modern antibiotic resistance dissemination through engineered systems. Our findings
464 highlight the need to consider AMR emergence as an integral component of the design and
465 operation of biological wastewater treatment processes.

466 **Associated content**

467 **Supporting Information**

468 All the supplementary methods, tables and figures are provided in Supporting Information.pdf.
469 Additionally, detailed information on differentially abundant ARGs, ARG family and drug
470 classes, and ARG correlation with ROS genes are provided in Supporting Data.xlsx.

471 **Author information**

472 **Corresponding Author**

473 **Naresh Singhal* Phone: +64 9 923 4512; e-mail:** n.singhal@auckland.ac.nz

474 **ORCID**

Bharat Manna: 0000-0001-7394-8204

Naresh Singhal: 0000-0002-9461-688X

Xueyang Zhou: 0000-0003-2591-0783

CRediT authorship contribution statement

BM: Conceptualization, Investigation, Methodology, Formal Analysis, Writing - original draft. XZ: Investigation, Methodology, Writing - review & editing. NS: Conceptualization, Funding acquisition, Supervision, Writing - review & editing.

Funding Sources

The study was funded by Marsden Award from the Royal Society of New Zealand (Contract Number: MFP-UOA2018) made to NS.

Notes

The authors declare no competing financial interest.

Acknowledgment

The authors acknowledge the use of New Zealand eScience Infrastructure (NeSI) high performance computing facilities, consulting support and/or training services as part of this research. New Zealand's national facilities are provided by NeSI and funded jointly by NeSI's collaborator institutions and through the Ministry of Business, Innovation & Employment's Research Infrastructure programme. URL https://www.nesi.org.nz. The authors also acknowledge the Centre for eResearch at the University of Auckland for their help in facilitating this research. http://www.eresearch.auckland.ac.nz.

REFERENCES

Agga, G.E., Arthur, T.M., Durso, L.M., Harhay, D.M., Schmidt, J.W., 2015. Antimicrobial-resistant bacterial populations and antimicrobial resistance genes obtained from environments impacted by livestock and municipal waste. PLoS One. https://doi.org/10.1371/journal.pone.0132586

Alcock, B.P., Raphenya, A.R., Lau, T.T.Y., Tsang, K.K., Bouchard, M., Edalatmand, A., Huynh, W., others, 2020. CARD 2020: Antibiotic resistome surveillance with the comprehensive antibiotic resistance database. Nucleic Acids Res. https://doi.org/10.1093/nar/gkz935

503 Alexander, J., Hembach, N., Schwartz, T., 2020. Evaluation of antibiotic resistance
504 dissemination by wastewater treatment plant effluents with different catchment areas in
505 Germany. Sci. Rep. https://doi.org/10.1038/s41598-020-65635-4

506 Ariza, R.R., Cohen, S.P., Bachhawat, N., Levy, S.B., Demple, B., 1994. Repressor mutations in
507 the marRAB operon that activate oxidative stress genes and multiple antibiotic resistance in
508 Escherichia coli. J. Bacteriol. https://doi.org/10.1128/jb.176.1.143-148.1994

509 Bengtsson-Palme, J., Hammarén, R., Pal, C., Östman, M., Björlenius, B., Flach, C.F., Fick, J.,
510 Kristiansson, E., Tysklind, M., Larsson, D.G.J., 2016. Elucidating selection processes for
511 antibiotic resistance in sewage treatment plants using metagenomics. Sci. Total Environ.
512 https://doi.org/10.1016/j.scitotenv.2016.06.228

513 Bolger, A.M., Lohse, M., Usadel, B., 2014. Trimmomatic: A flexible trimmer for Illumina
514 sequence data. Bioinformatics. https://doi.org/10.1093/bioinformatics/btu170

515 Buchfink, B., Xie, C., Huson, D.H., 2014. Fast and sensitive protein alignment using
516 DIAMOND. Nat. Methods. https://doi.org/10.1038/nmeth.3176

517 Centers, U.S., Control, D., Fattouh, M., El-Din, A.N., Davies, J., 2019. Centers for Disease
518 Control and Prevention. Antibiotic resistance threats in the United States, 2019. Int. J. Curr.
519 Microbiol. Appl. Sci.

520 Chen, C., Chen, H., Zhang, Y., Thomas, H.R., Frank, M.H., He, Y., Xia, R., 2020. TBtools: An
521 Integrative Toolkit Developed for Interactive Analyses of Big Biological Data. Mol. Plant.
522 https://doi.org/10.1016/j.molp.2020.06.009

523 Chen, Y., Shen, W., Wang, B., Zhao, X., Su, L., Kong, M., Li, H., Zhang, S., Li, J., 2020.
524 Occurrence and fate of antibiotics, antimicrobial resistance determinants and potential
525 human pathogens in a wastewater treatment plant and their effects on receiving waters in
526 Nanjing, China. Ecotoxicol. Environ. Saf. https://doi.org/10.1016/j.ecoenv.2020.111371

527 Christodoulou, D., Link, H., Fuhrer, T., Kochanowski, K., Gerosa, L., Sauer, U., 2018. Reserve
528 Flux Capacity in the Pentose Phosphate Pathway Enables Escherichia coli's Rapid
529 Response to Oxidative Stress. Cell Syst. https://doi.org/10.1016/j.cels.2018.04.009

530 Dcosta, V.M., King, C.E., Kalan, L., Morar, M., Sung, W.W.L., Schwarz, C., Froese, D., Zazula,
531 G., Calmels, F., Debruyne, R., Golding, G.B., Poinar, H.N., Wright, G.D., 2011. Antibiotic
532 resistance is ancient. Nature. https://doi.org/10.1038/nature10388

533 Dhariwal, A., Chong, J., Habib, S., King, I.L., Agellon, L.B., Xia, J., 2017. MicrobiomeAnalyst:
534 A web-based tool for comprehensive statistical, visual and meta-analysis of microbiome
535 data. Nucleic Acids Res. https://doi.org/10.1093/nar/gkx295

536 Dwyer, D.J., Kohanski, M.A., Collins, J.J., 2009. Role of reactive oxygen species in antibiotic
537 action and resistance. Curr. Opin. Microbiol. https://doi.org/10.1016/j.mib.2009.06.018

538 Garner, E., Maile-Moskowitz, A., Angeles, L.F., Flach, C.-F., Aga, D.S., Nambi, I., Larsson,

539 D.G.J., Bürgmann, H., Zhang, T., Vikesland, P.J., Pruden, A., 2024. Metagenomic Profiling
540 of Internationally Sourced Sewage Influents and Effluents Yields Insight into Selecting
541 Targets for Antibiotic Resistance Monitoring. Environ. Sci. \& Technol. 58, 16547–16559.

542 Guo, J., Li, J., Chen, H., Bond, P.L., Yuan, Z., 2017. Metagenomic analysis reveals wastewater
543 treatment plants as hotspots of antibiotic resistance genes and mobile genetic elements.
544 Water Res. https://doi.org/10.1016/j.watres.2017.07.002

545 Hocquet, D., Muller, A., Bertrand, X., 2016. What happens in hospitals does not stay in
546 hospitals: antibiotic-resistant bacteria in hospital wastewater systems. J. Hosp. Infect.
547 https://doi.org/10.1016/j.jhin.2016.01.010

548 Honda, R., Matsuura, N., Sorn, S., Asakura, S., Morinaga, Y., Van Huy, T., Sabar, M.A.,
549 Masakke, Y., Hara-Yamamura, H., Watanabe, T., 2023. Transition of antimicrobial
550 resistome in wastewater treatment plants: impact of process configuration, geographical
551 location and season. npj Clean Water. https://doi.org/10.1038/s41545-023-00261-x

552 Hyatt, D., Chen, G.L., LoCascio, P.F., Land, M.L., Larimer, F.W., Hauser, L.J., 2010. Prodigal:
553 Prokaryotic gene recognition and translation initiation site identification. BMC
554 Bioinformatics. https://doi.org/10.1186/1471-2105-11-119

555 Imlay, J.A., 2019. Where in the world do bacteria experience oxidative stress? Environ.
556 Microbiol. https://doi.org/10.1111/1462-2920.14445

557 Imlay, J.A., 2008. Cellular defenses against superoxide and hydrogen peroxide. Annu. Rev.
558 Biochem. https://doi.org/10.1146/annurev.biochem.77.061606.161055

559 Imlay, J.A., 2003. Pathways of Oxidative Damage. Annu. Rev. Microbiol.
560 https://doi.org/10.1146/annurev.micro.57.030502.090938

561 Itzek, A., Zheng, L., Chen, Z., Merritt, J., Kreth, J., 2011. Hydrogen peroxide-dependent DNA
562 release and transfer of antibiotic resistance genes in Streptococcus gordonii. J. Bacteriol.
563 https://doi.org/10.1128/JB.05791-11

564 Jin, M., Lu, J., Chen, Z., Nguyen, S.H., Mao, L., Li, J., Yuan, Z., Guo, J., 2018. Antidepressant
565 fluoxetine induces multiple antibiotics resistance in Escherichia coli via ROS-mediated
566 mutagenesis. Environ. Int. https://doi.org/10.1016/j.envint.2018.07.046

567 Ju, F., Beck, K., Yin, X., Maccagnan, A., McArdell, C.S., Singer, H.P., Johnson, D.R., Zhang,
568 T., Bürgmann, H., 2019. Wastewater treatment plant resistomes are shaped by bacterial
569 composition, genetic exchange, and upregulated expression in the effluent microbiomes.
570 ISME J. https://doi.org/10.1038/s41396-018-0277-8

571 Kanehisa, M., Goto, S., 2000. KEGG: Kyoto Encyclopedia of Genes and Genomes. Nucleic
572 Acids Res. https://doi.org/10.1093/nar/28.1.27

573 Karkman, A., Do, T.T., Walsh, F., Virta, M.P.J., 2018. Antibiotic-Resistance Genes in Waste
574 Water. Trends Microbiol. https://doi.org/10.1016/j.tim.2017.09.005

575 Kohanski, M.A., Dwyer, D.J., Wierzbowski, J., Cottarel, G., Collins, J.J., 2008. Mistranslation of
576 Membrane Proteins and Two-Component System Activation Trigger Antibiotic-Mediated
577 Cell Death. Cell. https://doi.org/10.1016/j.cell.2008.09.038

578 Korzeniewska, E., Korzeniewska, A., Harnisz, M., 2013. Antibiotic resistant Escherichia coli in
579 hospital and municipal sewage and their emission to the environment. Ecotoxicol. Environ.
580 Saf. https://doi.org/10.1016/j.ecoenv.2013.01.014

581 Lam, P.L., Wong, R.S.M., Lam, K.H., Hung, L.K., Wong, M.M., Yung, L.H., Ho, Y.W., Wong,
582 W.Y., Hau, D.K.P., Gambari, R., Chui, C.H., 2020. The role of reactive oxygen species in
583 the biological activity of antimicrobial agents: An updated mini review. Chem. Biol.
584 Interact. https://doi.org/10.1016/j.cbi.2020.109023

585 Lau, G.W., Britigan, B.E., Hassett, D.J., 2005. Pseudomonas aeruginosa OxyR is required for
586 full virulence in rodent and insect models of infection and for resistance to human
587 neutrophils. Infect. Immun. https://doi.org/10.1128/IAI.73.4.2550-2553.2005

588 Lemire, J., Alhasawi, A., Appanna, V.P., Tharmalingam, S., Appanna, V.D., 2017. Metabolic
589 defence against oxidative stress: the road less travelled so far. J. Appl. Microbiol.
590 https://doi.org/10.1111/jam.13509

591 Li, B., Yang, Y., Ma, L., Ju, F., Guo, F., Tiedje, J.M., Zhang, T., 2015. Metagenomic and
592 network analysis reveal wide distribution and co-occurrence of environmental antibiotic
593 resistance genes. ISME J. https://doi.org/10.1038/ismej.2015.59

594 Li, D., Liu, C.M., Luo, R., Sadakane, K., Lam, T.W., 2015. MEGAHIT: An ultra-fast single-
595 node solution for large and complex metagenomics assembly via succinct de Bruijn graph.
596 Bioinformatics. https://doi.org/10.1093/bioinformatics/btv033

597 Li, H., Zhou, X., Huang, Y., Liao, B., Cheng, L., Ren, B., 2021. Reactive Oxygen Species in
598 Pathogen Clearance: The Killing Mechanisms, the Adaption Response, and the Side Effects.
599 Front. Microbiol. https://doi.org/10.3389/fmicb.2020.622534

600 Lira, F., Vaz-Moreira, I., Tamames, J., Manaia, C.M., Martínez, J.L., 2020. Metagenomic
601 analysis of an urban resistome before and after wastewater treatment. Sci. Rep.
602 https://doi.org/10.1038/s41598-020-65031-y

603 Liu, S.S., Qu, H.M., Yang, D., Hu, H., Liu, W.L., Qiu, Z.G., Hou, A.M., Guo, J., Li, J.W., Shen,
604 Z.Q., Jin, M., 2018. Chlorine disinfection increases both intracellular and extracellular
605 antibiotic resistance genes in a full-scale wastewater treatment plant. Water Res.
606 https://doi.org/10.1016/j.watres.2018.02.036

607 Liu, Z., Klümper, U., Liu, Y., Yang, Y., Wei, Q., Lin, J.G., Gu, J.D., Li, M., 2019. Metagenomic
608 and metatranscriptomic analyses reveal activity and hosts of antibiotic resistance genes in
609 activated sludge. Environ. Int. https://doi.org/10.1016/j.envint.2019.05.036

610 Luo, L., Yao, J., Liu, W., Yang, L., Li, H., Liang, M., Ma, H., Liu, Z., Chen, Y., 2021.
611 Comparison of bacterial communities and antibiotic resistance genes in oxidation ditches

612 and membrane bioreactors. Sci. Rep. https://doi.org/10.1038/s41598-021-88335-z

613 Lyons, T.W., Reinhard, C.T., Planavsky, N.J., 2014. The rise of oxygen in Earth's early ocean
614 and atmosphere. Nature. https://doi.org/10.1038/nature13068

615 Lyu, F., Han, F., Ge, C., Mao, W., Chen, L., Hu, H., Chen, G., Lang, Q., Fang, C., 2023.
616 OmicStudio: A composable bioinformatics cloud platform with real-time feedback that can
617 generate high-quality graphs for publication. iMeta. https://doi.org/10.1002/imt2.85

618 Ma, X., Zhang, Xiuwen, Xia, J., Sun, H., Zhang, Xuxiang, Ye, L., 2021. Phenolic compounds
619 promote the horizontal transfer of antibiotic resistance genes in activated sludge. Sci. Total
620 Environ. https://doi.org/10.1016/j.scitotenv.2021.149549

621 Majeed, H.J., Riquelme, M. V., Davis, B.C., Gupta, S., Angeles, L., Aga, D.S., Garner, E.,
622 Pruden, A., Vikesland, P.J., 2021. Evaluation of Metagenomic-Enabled Antibiotic
623 Resistance Surveillance at a Conventional Wastewater Treatment Plant. Front. Microbiol.
624 https://doi.org/10.3389/fmicb.2021.657954

625 Manaia, C.M., Rocha, J., Scaccia, N., Marano, R., Radu, E., Biancullo, F., Cerqueira, F.,
626 Fortunato, G., Iakovides, I.C., Zammit, I., Kampouris, I., Vaz-Moreira, I., Nunes, O.C.,
627 2018. Antibiotic resistance in wastewater treatment plants: Tackling the black box. Environ.
628 Int. https://doi.org/10.1016/j.envint.2018.03.044

629 Mandsberg, L.F., Ciofu, O., Kirkby, N., Christiansen, L.E., Poulsen, H.E., Høiby, N., 2009.
630 Antibiotic resistance in Pseudomonas aeruginosa strains with increased mutation frequency
631 due to inactivation of the DNA oxidative repair system. Antimicrob. Agents Chemother.
632 https://doi.org/10.1128/AAC.00428-08

633 Manna, B., Jay, E., Zhang, W., Zhou, X., Lyu, B., Thomas, G.M., Singhal, N., 2024. Short-Term
634 Warming Induces Cyanobacterial Blooms and Antibiotic Resistance in Freshwater Lake, as
635 Revealed by Metagenomics Analysis. Water 16, 2655.

636 McEwen, S.A., Collignon, P.J., 2018. Antimicrobial Resistance: a One Health Perspective.
637 Microbiol. Spectr. https://doi.org/10.1128/microbiolspec.arba-0009-2017

638 Mehanni, M.M., Gadow, S.I., Alshammari, F.A., Modafer, Y., Ghanem, K.Z., El-Tahtawi, N.F.,
639 El-Homosy, R.F., Hesham, A.E.L., 2023. Antibiotic-resistant bacteria in hospital
640 wastewater treatment plant effluent and the possible consequences of its reuse in
641 agricultural irrigation. Front. Microbiol. https://doi.org/10.3389/fmicb.2023.1141383

642 Murray, Christopher JL, et al., 2022. Global burden of bacterial antimicrobial resistance in
643 2019: a systematic analysis. Lancet. https://doi.org/10.1016/S0140-6736(21)02724-0

644 Muth, T., Behne, A., Heyer, R., Kohrs, F., Benndorf, D., Hoffmann, M., Lehtevä, M., Reichl, U.,
645 Martens, L., Rapp, E., 2015. The MetaProteomeAnalyzer: A powerful open-source software
646 suite for metaproteomics data analysis and interpretation. J. Proteome Res.
647 https://doi.org/10.1021/pr501246w

648 Nelson, R.E., Hatfield, K.M., Wolford, H., Samore, M.H., Scott, R.D., Reddy, S.C., Olubajo, B.,
649 Paul, P., Jernigan, J.A., Baggs, J., 2021. National estimates of healthcare costs associated
650 with multidrug-resistant bacterial infections among hospitalized patients in the United
651 States. Clin. Infect. Dis. https://doi.org/10.1093/cid/ciaa1581

652 Paulus, G.K., Hornstra, L.M., Alygizakis, N., Slobodnik, J., Thomaidis, N., Medema, G., 2019.
653 The impact of on-site hospital wastewater treatment on the downstream communal
654 wastewater system in terms of antibiotics and antibiotic resistance genes. Int. J. Hyg.
655 Environ. Health. https://doi.org/10.1016/j.ijheh.2019.01.004

656 Petrovich, M.L., Zilberman, A., Kaplan, A., Eliraz, G.R., Wang, Y., Langenfeld, K., Duhaime,
657 M., Wigginton, K., Poretsky, R., Avisar, D., Wells, G.F., 2020. Microbial and Viral
658 Communities and Their Antibiotic Resistance Genes Throughout a Hospital Wastewater
659 Treatment System. Front. Microbiol. https://doi.org/10.3389/fmicb.2020.00153

660 Puente-Sánchez, F., Garciá-Garciá, N., Tamames, J., 2020. SQMtools: Automated processing
661 and visual analysis of 'omics data with R and anvi'o. BMC Bioinformatics.
662 https://doi.org/10.1186/s12859-020-03703-2

663 Qi, W., Jonker, M.J., Teichmann, L., Wortel, M., ter Kuile, B.H., 2023. The influence of oxygen
664 and oxidative stress on de novo acquisition of antibiotic resistance in E. coli and
665 Lactobacillus lactis. BMC Microbiol. 23, 1–14. https://doi.org/10.1186/s12866-023-03031-
666 4

667 R Core Team, 2022. R Core Team 2021 R: A language and environment for statistical
668 computing. R foundation for statistical computing. https://www.R-project.org/. R Found.
669 Stat. Comput.

670 Robinson Mark, D., McCarthy Davis, J., Smyth Gordon, K., 2010. edgeR: a Bioconductor
671 package for differential expression analysis of digital gene expression data. Bioinformatics.

672 Rowe, W.P.M., Baker-Austin, C., Verner-Jeffreys, D.W., Ryan, J.J., Micallef, C., Maskell, D.J.,
673 Pearce, G.P., 2017. Overexpression of antibiotic resistance genes in hospital effluents over
674 time. J. Antimicrob. Chemother. https://doi.org/10.1093/jac/dkx017

675 Schneider, D., Aßmann, N., Wicke, D., Poehlein, A., Daniel, R., 2020. Metagenomes of
676 Wastewater at Different Treatment Stages in Central Germany. Microbiol. Resour.
677 Announc. https://doi.org/10.1128/mra.00201-20

678 Schneider, D., Zühlke, D., Poehlein, A., Riedel, K., Daniel, R., 2021. Metagenome-Assembled
679 Genome Sequences from Different Wastewater Treatment Stages in Germany. Microbiol.
680 Resour. Announc. https://doi.org/10.1128/mra.00504-21

681 Seemann, T., 2014. Prokka: Rapid prokaryotic genome annotation. Bioinformatics.
682 https://doi.org/10.1093/bioinformatics/btu153

683 Seo, S.W., Kim, D., Szubin, R., Palsson, B.O., 2015. Genome-wide Reconstruction of OxyR and
684 SoxRS Transcriptional Regulatory Networks under Oxidative Stress in Escherichia coli K-

12 MG1655. Cell Rep. https://doi.org/10.1016/j.celrep.2015.07.043

Sulfikar, Honda, R., Noguchi, M., Yamamoto-Ikemoto, R., Watanabe, T., 2018. Effect of sedimentation and aeration on antibiotic resistance induction in the activated sludge process. J. Water Environ. Technol. https://doi.org/10.2965/jwet.17-046

Tamames, J., Puente-Sánchez, F., 2019. SqueezeMeta, a highly portable, fully automatic metagenomic analysis pipeline. Front. Microbiol. https://doi.org/10.3389/fmicb.2018.03349

Tan, Q., Chen, J., Chu, Y., Liu, W., Yang, L., Ma, L., Zhang, Y., Qiu, D., Wu, Z., He, F., 2021. Triclosan weakens the nitrification process of activated sludge and increases the risk of the spread of antibiotic resistance genes. J. Hazard. Mater. https://doi.org/10.1016/j.jhazmat.2021.126085

Uluseker, C., Kaster, K.M., Thorsen, K., Basiry, D., Shobana, S., Jain, M., Kumar, G., Kommedal, R., Pala-Ozkok, I., 2021. A Review on Occurrence and Spread of Antibiotic Resistance in Wastewaters and in Wastewater Treatment Plants: Mechanisms and Perspectives. Front. Microbiol. https://doi.org/10.3389/fmicb.2021.717809

Van Acker, H., Coenye, T., 2017. The Role of Reactive Oxygen Species in Antibiotic-Mediated Killing of Bacteria. Trends Microbiol. https://doi.org/10.1016/j.tim.2016.12.008

Wang, P., Zhang, H., Liu, Y., Lv, R., Liu, X., Song, X., Wang, J., Jiang, L., 2020. SoxS is a positive regulator of key pathogenesis genes and promotes intracellular replication and virulence of Salmonella Typhimurium. Microb. Pathog. https://doi.org/10.1016/j.micpath.2019.103925

Wang, Y., Han, Y., Li, L., Liu, J., Yan, X., 2022. Distribution, sources, and potential risks of antibiotic resistance genes in wastewater treatment plant: A review. Environ. Pollut. https://doi.org/10.1016/j.envpol.2022.119870

Wang, Y., Lu, J., Engelstädter, J., Zhang, S., Ding, P., Mao, L., Yuan, Z., Bond, P.L., Guo, J., 2020. Non-antibiotic pharmaceuticals enhance the transmission of exogenous antibiotic resistance genes through bacterial transformation. ISME J. https://doi.org/10.1038/s41396-020-0679-2

Wei, Q., Le Minh, P.N., Dötsch, A., Hildebrand, F., Panmanee, W., Elfarash, A., Schulz, S., Plaisance, S., Charlier, D., Hassett, D., Häussler, S., Cornelis, P., 2012. Global regulation of gene expression by OxyR in an important human opportunistic pathogen. Nucleic Acids Res. https://doi.org/10.1093/nar/gks017

Wei, Z., Feng, K., Wang, Z., Zhang, Y., Yang, M., Zhu, Y.G., Virta, M.P.J., Deng, Y., 2021. High-Throughput Single-Cell Technology Reveals the Contribution of Horizontal Gene Transfer to Typical Antibiotic Resistance Gene Dissemination in Wastewater Treatment Plants. Environ. Sci. Technol. https://doi.org/10.1021/acs.est.1c01250

Wickham, H., 2011. ggplot2. Wiley Interdiscip. Rev. Comput. Stat. https://doi.org/10.1002/wics.147

722 Yang, J.H., Wright, S.N., Hamblin, M., McCloskey, D., Alcantar, M.A., Schrübbers, L.,
723 Lopatkin, A.J., Satish, S., Nili, A., Palsson, B.O., Walker, G.C., Collins, J.J., 2019. A
724 White-Box Machine Learning Approach for Revealing Antibiotic Mechanisms of Action.
725 Cell. https://doi.org/10.1016/j.cell.2019.04.016

726

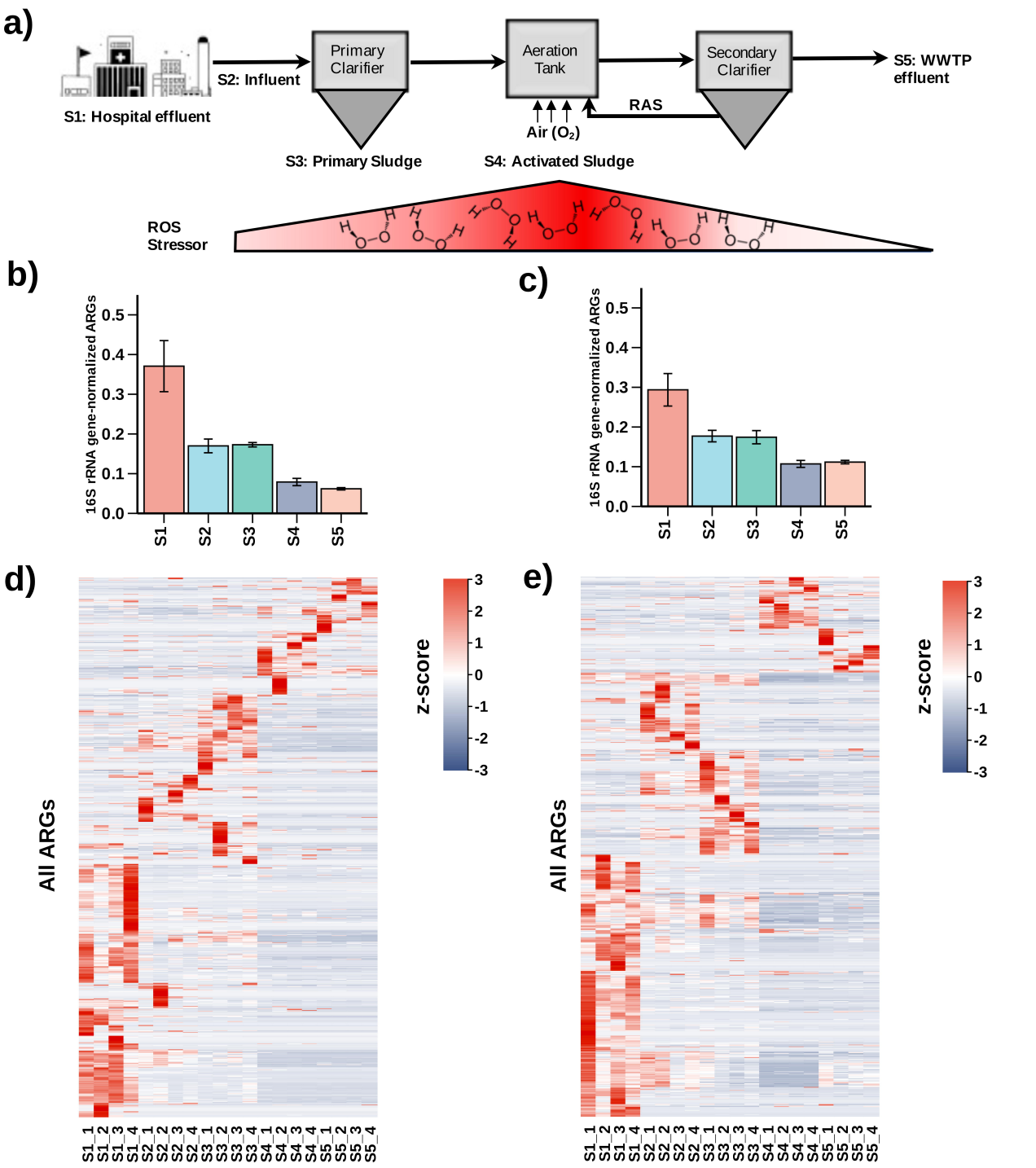
a)
S1: Hospital effluent
S2: Influent
Primary Clarifier
S3: Primary Sludge
Aeration Tank
Air (O2)
S4: Activated Sludge
RAS
Secondary Clarifier
S5: WWTP effluent
ROS Stressor
b)
16S rRNA gene-normalized ARGs
0.0
0.1
0.2
0.3
0.4
0.5
S1
S2
S3
S4
S5
c)
16S rRNA gene-normalized ARGs
0.0
0.1
0.2
0.3
0.4
0.5
S1
S2
S3
S4
S5
d)
All ARGs
z-score
3
2
1
0
-1
-2
-3
S1_1 S1_2 S1_3 S1_4 S2_1 S2_2 S2_3 S2_4 S3_1 S3_2 S3_3 S3_4 S4_1 S4_2 S4_3 S4_4 S5_1 S5_2 S5_3 S5_4
e)
All ARGs
z-score
3
2
1
0
-1
-2
-3
S1_1 S1_2 S1_3 S1_4 S2_1 S2_2 S2_3 S2_4 S3_1 S3_2 S3_3 S3_4 S4_1 S4_2 S4_3 S4_4 S5_1 S5_2 S5_3 S5_4

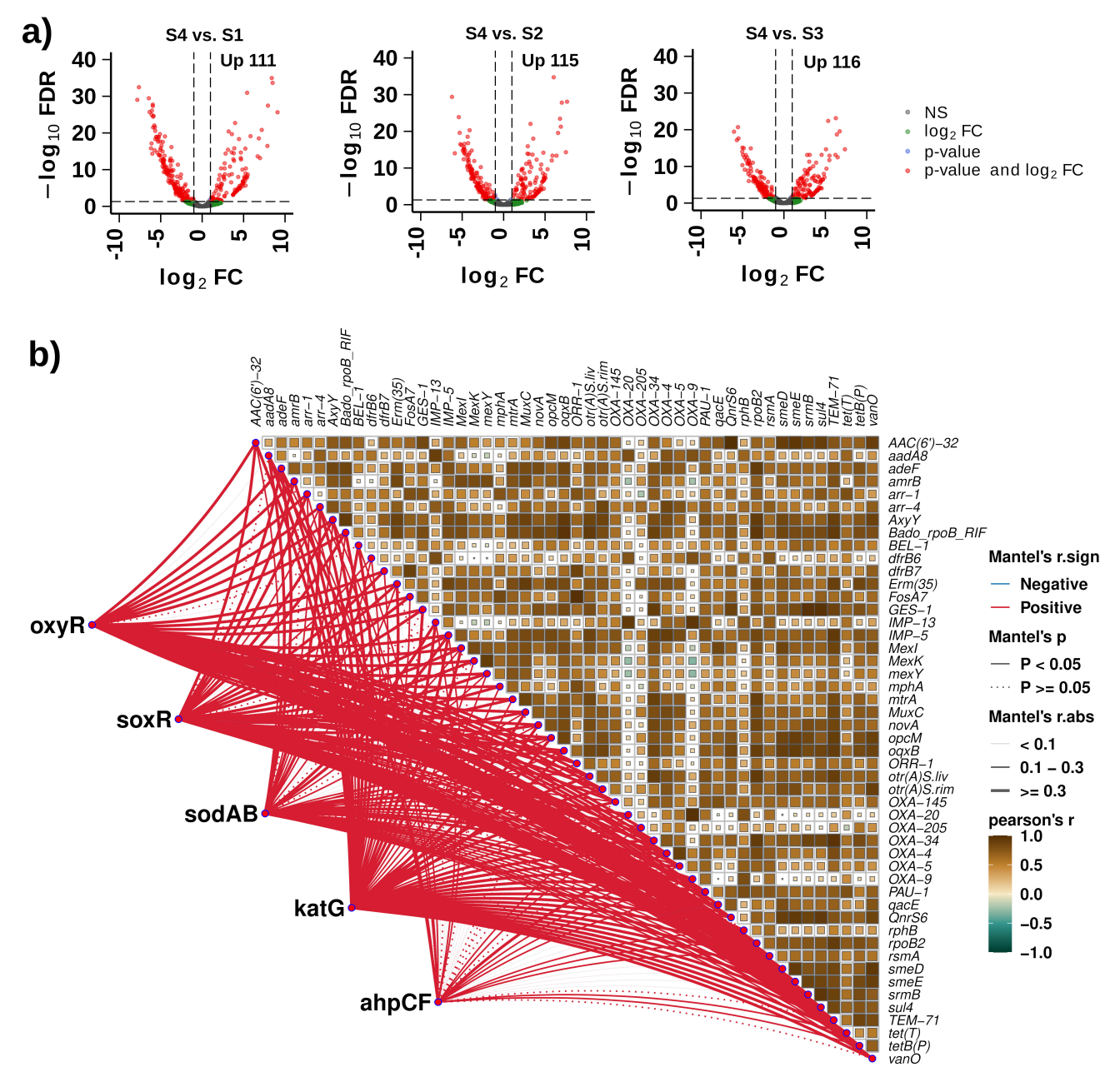
a)
S4 vs. S1
Up 111
S4 vs. S2
Up 115
S4 vs. S3
Up 116
−log10 FDR
log2 FC
NS
log2 FC
p-value
p-value and log2 FC
b)
oxyR
soxR
sodAB
katG
ahpCF
AAC(6')−32
aadA8
adeF
amrB
arr−1
arr−4
AxyY
Bado_rpoB_RIF
BEL−1
dfrB6
dfrB7
Erm(35)
FosA7
GES−1
IMP−13
IMP−5
MexI
MexK
mexY
mphA
mtrA
MuxC
novA
opcM
oqxB
ORR−1
otr(A)S.liv
otr(A)S.rim
OXA−145
OXA−20
OXA−205
OXA−34
OXA−4
OXA−5
OXA−9
PAU−1
qacE
QnrS6
rphB
rpoB2
rsmA
smeD
smeE
srmB
sul4
TEM−71
tet(T)
tetB(P)
vanO
Mantel's r.sign
Negative
Positive
Mantel's p
P < 0.05
P >= 0.05
Mantel's r.abs
< 0.1
0.1 – 0.3
>= 0.3
pearson's r
1.0
0.5
0.0
−0.5
−1.0

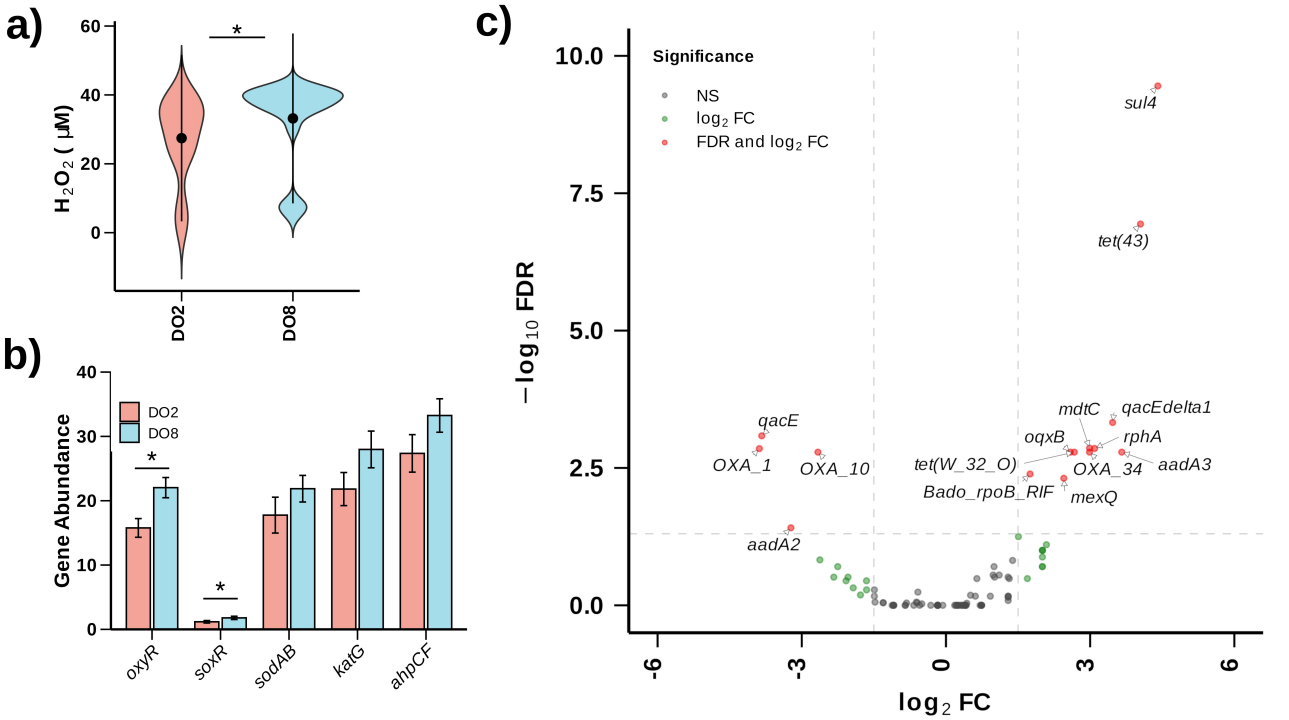
a)
60
40
20
0
*
H_2O_2 (μM)
DO2
DO8
b)
40
30
20
10
0
Gene Abundance
DO2
DO8
*
*
oxyR
soxR
sodAB
katG
ahpCF
c)
Significance
NS
log_2 FC
FDR and log_2 FC
10.0
7.5
5.0
2.5
0.0
$-log_{10}$ FDR
sul4
tet(43)
qacE
OXA_1
OXA_10
aadA2
mdtC
qacEdelta1
oqxB
rphA
tet(W_32_O)
OXA_34
aadA3
Bado_rpoB_RIF
mexQ
-6
-3
0
3
6
log_2 FC

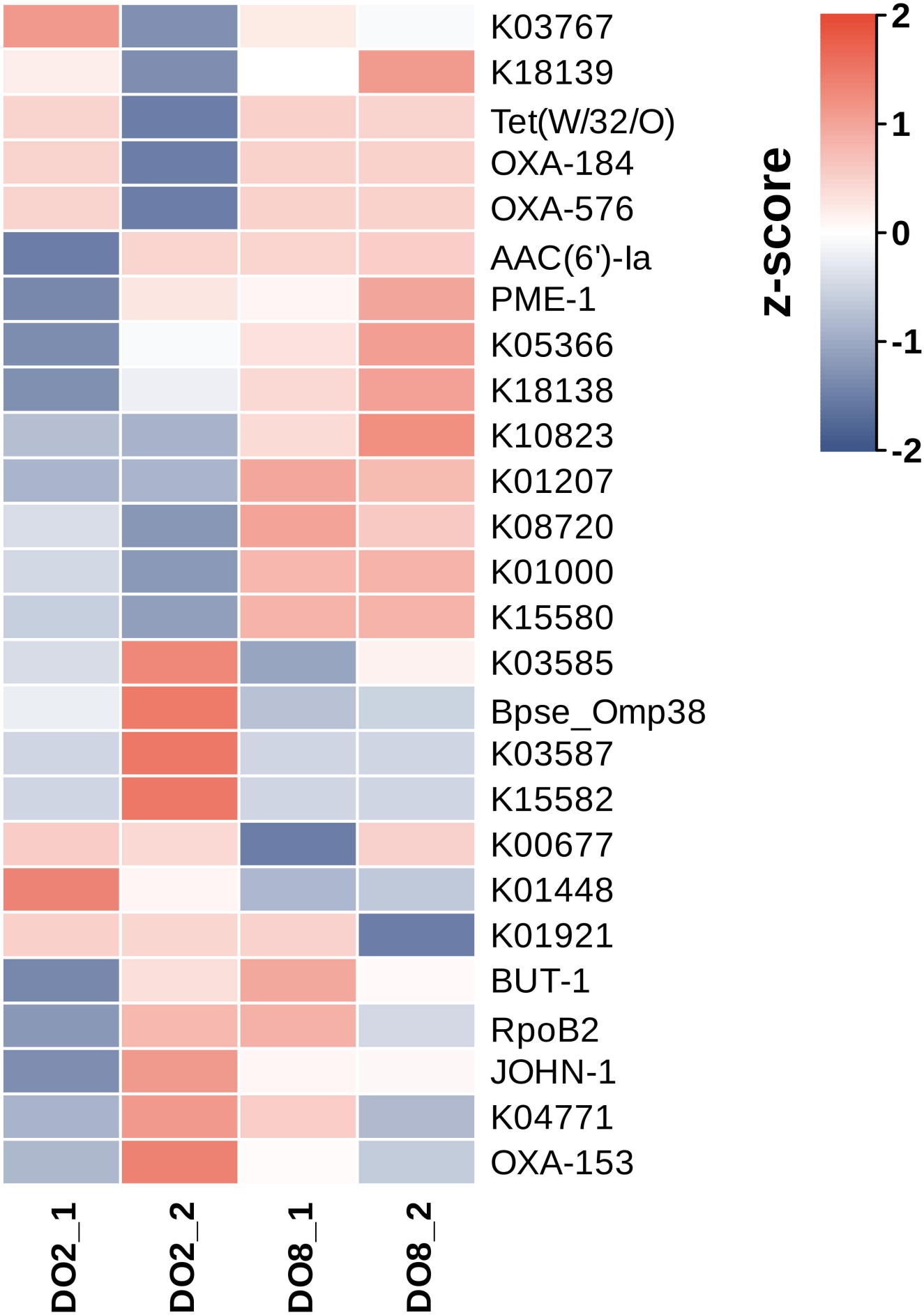
K03767
K18139
Tet(W/32/O)
OXA-184
OXA-576
AAC(6')-Ia
PME-1
K05366
K18138
K10823
K01207
K08720
K01000
K15580
K03585
Bpse_Omp38
K03587
K15582
K00677
K01448
K01921
BUT-1
RpoB2
JOHN-1
K04771
OXA-153
DO2_1
DO2_2
DO8_1
DO8_2
z-score
2
1
0
-1
-2

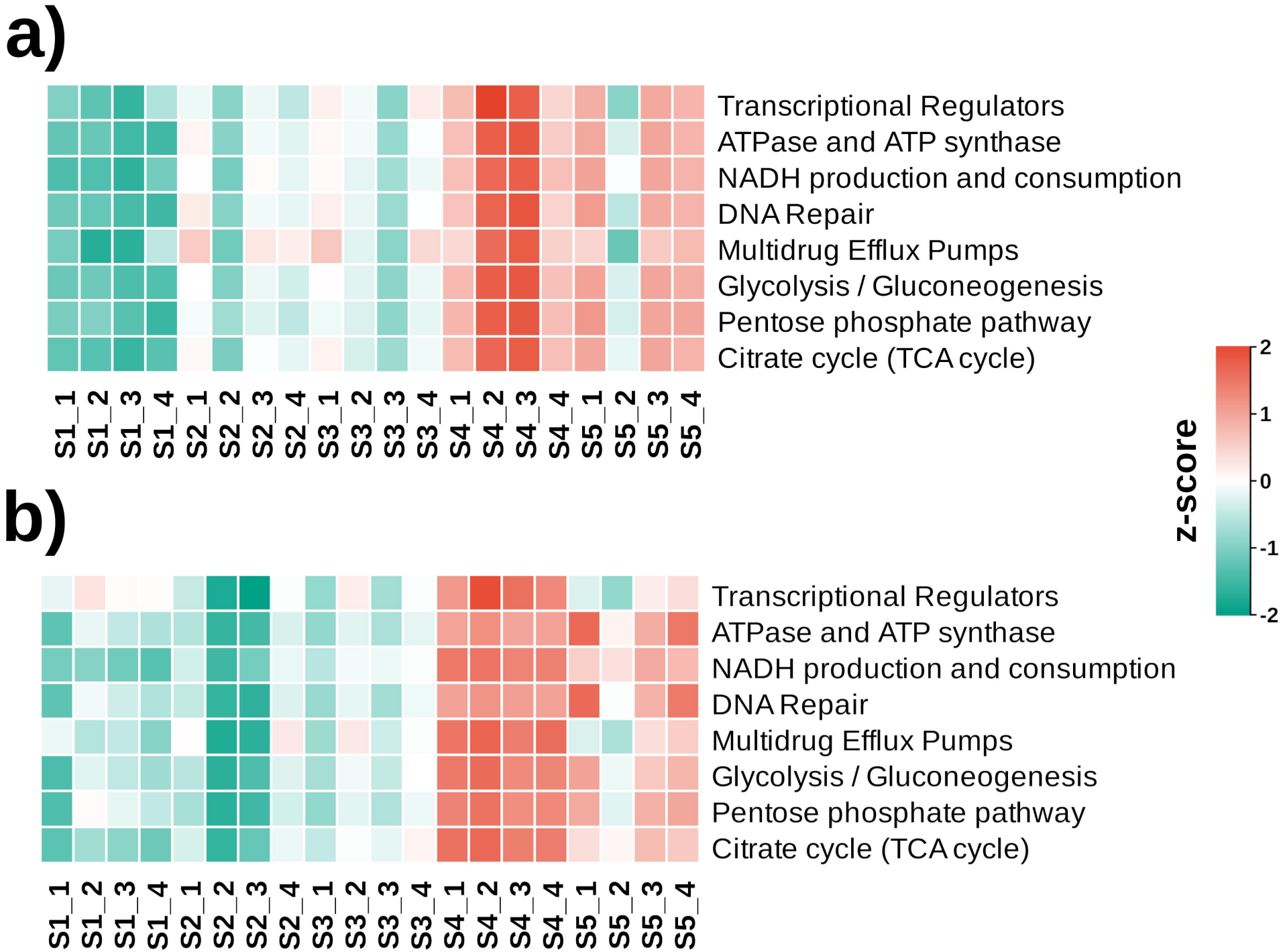
a)
Transcriptional Regulators
ATPase and ATP synthase
NADH production and consumption
DNA Repair
Multidrug Efflux Pumps
Glycolysis / Gluconeogenesis
Pentose phosphate pathway
Citrate cycle (TCA cycle)
S1_1 S1_2 S1_3 S1_4 S2_1 S2_2 S2_3 S2_4 S3_1 S3_2 S3_3 S3_4 S4_1 S4_2 S4_3 S4_4 S5_1 S5_2 S5_3 S5_4
b)
Transcriptional Regulators
ATPase and ATP synthase
NADH production and consumption
DNA Repair
Multidrug Efflux Pumps
Glycolysis / Gluconeogenesis
Pentose phosphate pathway
Citrate cycle (TCA cycle)
S1_1 S1_2 S1_3 S1_4 S2_1 S2_2 S2_3 S2_4 S3_1 S3_2 S3_3 S3_4 S4_1 S4_2 S4_3 S4_4 S5_1 S5_2 S5_3 S5_4
z-score
2
1
0
-1
-2